International Journal of Environmental Science and Technology (2020) 17:3761–3770
https://doi.org/10.1007/s13762-020-02732-x

ORIGINAL PAPER

Effective removal of *Microcystis aeruginosa* and microcystins by integrated pre-oxidation and coagulation: an environmental and economical way

Q. Song[1] · D. Zhang[5] · X. Niu[1,2,3,4,5] · Y. Li[1] · J. Ma[1] · Y. Fan[1] · S. Zhou[1]

Received: 4 November 2019 / Revised: 25 March 2020 / Accepted: 31 March 2020 / Published online: 18 April 2020

Abstract

The frequent occurrence of cyanobacteria blooms has gained worldwide concern. The conventional pre-oxidation methods are not only less effective in removing *Microcystis aeruginosa* cells, but also tend to trigger secondary pollution with an inevitable release of intracellular organic matter. In this study, Fe^{2+}/persulfate process was applied to generate sulfate radicals and simultaneously form in situ Fe (III) for integrated oxidation–coagulation, leading to a notable enhancement in *M. aeruginosa* removal without cell breakage and better control of microcystins. Results showed that the Fe^{2+}/persulfate mass ratio of 1:1 and the $FeSO_4$ dosage of 0.1 mmol/L were efficient in *M. aeruginosa* removal. With the optimal $FeSO_4$ dosage, up to 90.1% of *M. aeruginosa* were removed intact with the cell zeta potential of − 0.814. After settling down of *M. aeruginosa* within 30 min, the chlorophyll-a removal efficiency reached 98.9% and microcystins decreased remarkably. Furthermore, the degradation of algal organic matters was significantly enhanced with a relatively lower residual Fe. Protein-like substances and dissolved microbial metabolites were preferentially oxidized. The cell lysis only occurred to a small number of *M. aeruginosa* during the Fe^{2+}/persulfate process, preventing from the environmental risk posed. This work demonstrates that an appropriate Fe^{2+}/persulfate ratio and $FeSO_4$ addition is a feasible and promising method for removing *M. aeruginosa* in an environmental-friendly and cost-effective way.

Keywords Algal organic matters · Cell damage · Cyanobacteria · Fe^{2+}/persulfate · Integrated pre-oxidation and coagulation

Editorial responsibility: Josef Trögl.

Electronic supplementary material The online version of this article (https://doi.org/10.1007/s13762-020-02732-x) contains supplementary material, which is available to authorized users.

✉ X. Niu
xjniu@scut.edu.cn

[1] School of Environment and Energy, South China University of Technology, Guangzhou Higher Education Mega Center, 382 Waihuan East Road, Guangzhou 510006, China

[2] State Key Laboratory of Lake Science and Environment, Nanjing Institute of Geography and Limnology, Chinese Academy of Sciences, Nanjing 210008, China

[3] State Key Laboratory of Pollution Control and Resource Reuse, Nanjing 210093, China

[4] Guangdong Provincial Key Laboratory of Atmospheric Environment and Pollution Control, Guangzhou 510640, China

[5] School of Environmental Science and Engineering, Guangdong University of Petrochemical Technology, Maoming 525000, China

Introduction

The cyanobacteria bloom has frequently occurred in various types of surface water and caused serious problems for drinking water supply (Henderson et al. 2008). The excessive growth of toxic cyanobacteria has become a notorious environmental phenomenon and posed a threat to aquatic ecosystems, due to their blooming deteriorated water quality subject to prevalent eutrophication (Min et al. 2008; Paerl and Paul 2012; Sun et al. 2012). As one of the typical toxin-producing and dominant cyanobacteria, *Microcystis aeruginosa* can excrete algal organic matters (AOM) during the exponential growth phase, such as intracellular organic matters (IOMs), extracellular organic matters (EOMs), precursors of disinfection by-products (DBPs), taste and odor substances, as well as microcystins (MCs). The AOM tended to release from the cells of *M. aeruginosa* under environmental stress responsible for cell lysis (Lei et al. 2012; Svrcek and Smith 2004). The accelerated mass release of AOM enhanced the stability of *M. aeruginosa* cell, making

M. aeruginosa removal more difficult than an intact whole cell. Therefore, effective strategies are imperatively needed for enhancing the control of *M. aeruginosa* by decomposing the AOM without damaging cell integrity and causing metabolites releasing.

Oxidation and coagulation are common methods for removing cyanobacteria cells due to their high efficiency and excellent performance. The conventional coagulation has difficulty in complete removal of *M. aeruginosa* cells, because *M. aeruginosa* cells possess negatively charged structure nature with high mobility and diverse morphology (Ma et al. 2012a, b; Pieterse and Cloot 1997; Teixeira and Rosa 2006). The excretion of dissolved AOM from cell metabolism can form a protective shield to *M. aeruginosa* cells and make the removal of *M. aeruginos*a even more difficult (Ma et al. 2016). Furthermore, the addition of various oxidants prior to coagulation, such as chlorine, chlorine dioxide, ozone, potassium permanganate and potassium ferrate, has been widely applied for the removal of cyanobacterial cells (He and Wert 2016; Ma et al. 2012a, b; Zhao and Zhang 2011; Zhou et al. 2014). However, some oxidants (e.g., ozone, chlorine dioxide) may have negative effects on coagulation, due to the excessive oxidation, resulting in cyanobacterial cell lysis and IOM release. With the inevitable release of undesirable dissolved toxins, AOM degradation associated with forming low molecular weight (MW) compounds may make the coagulation process more challenging (Lei et al. 2012).

Recently, advanced oxidation processes (AOPs), such as hydroxyl radical ($OH^{\cdot}$) and sulfate radicals ($SO_4^{\cdot-}$), have been applied widely as promising options for degradation and mineralization of microorganic pollutants (Kwon et al. 2015). The $SO_4^{\cdot-}$ can be formed by persulfate (e.g., PS, $S_2O_8^{2-}$) or peroxymonosulfate (e.g., PMS, HSO_5^{-}) in various activation ways, such as heat (Hisao et al. 2008), alkaline (Qi et al. 2016), UV (Mahdiahmed and Chiron 2014) and transition metal (Rodriguez et al. 2014). Compared to $OH^{\cdot}$, the selectivity, redox potential and half-life of $SO_4^{\cdot-}$ were high (Ahmed et al. 2012; Wang and Wang 2018). In previous studies, UV-activated persulfate was found to significantly improve the removal efficiency of *M. aeruginosa* cells up to 98.2%, compared to employing UV inactivation alone, while at the same time it might cause complete *M. aeruginosa* cell lysis and damage, posing environmental risk for producing IOM, a secondary pollutant (Wang et al. 2016). Similarly, Jia et al. (2017) reported that UV/H_2O_2-generated $OH^{\cdot}$ from pre-oxidation could enhance the coagulation of *M. aeruginosa* from Fe (II) with the removal efficiency of 94.7%. However, additional coagulants (e.g., Al^{3+}, Fe^{3+}) were also introduced to the coagulation process, resulting in sever cell lysis with secondary environmental pollutions. Those pre-oxidation processes are relatively independent and separate to subsequent coagulation process, which possess higher potential dangers owing to a longer contact time. Besides, it has been well documented that the cell damage was rarely observed in the coagulation process with potassium ferrate (VI); however, the removal efficiency of *M. aeruginosa* was rather poor (Zhou et al. 2014). Fe (II) /PMS has been proved to remove *M. aeruginosa* cell efficiently with a moderate cell lysis (Zhou et al. 2020); however, the instability of PMS in natural water impeded its wide application. Therefore, the strategies for enhancing the removal efficiency of *M. aeruginosa* without cell damage are highly desired in an environmental and economical way.

In this study, the oxidation with Fe^{2+} activated persulfate (i.e., PS, $S_2O_8^{2-}$) to generate $SO_4^{\cdot-}$ was applied to remove *M. aeruginosa* without additional coagulants and serious cell lysis. The main objective of this study is to moderate the oxidation processes and simultaneously form in situ Fe (III) as coagulants to control AOM as well as *M. aeruginosa*. More specially, this study is aimed to: (1) determine the optimal concentration of $FeSO_4$ and $Na_2S_2O_8$ for *M. aeruginosa* removal and simultaneously maintaining cell integrity; (2) identify the cell structure and the characteristics of AOM; and (3) investigate the possible mechanisms involved in the pre-oxidation and coagulation process. This study was carried out in the laboratories of School of Environment and Energy, South China University of Technology, Guangzhou, China, in 2018.

Materials and methods

Materials and reagents

Microcystis aeruginosa FACHB-905 was obtained from the Institute of Hydrobiology, Chinese Academy of Science, and cultured in BG11 media. The cultures were incubated at 25 °C under illumination (2500 lx) with a 12 h light/12 h dark cycle in powder BG11 medium (Qingdao Haibo Institute of Biology) (Sheng et al. 2019). *M. aeruginosa* cells in late exponential growth phase were harvested and diluted by Milli-Q water to achieve a final cell density of 1.0×10^6 cells/mL (Gu et al. 2017). Afterward, the pH of *M. aeruginosa* solution was adjusted to 7.5 approaching ambient environment with 0.1 mmol/L H_2SO_4 and 0.1 mmol/L NaOH.

All the chemicals used were analytical grade. Ferrous sulfate ($FeSO_4$), sodium sulfate ($Na_2S_2O_8$), NaOH (≥ 98%), H_2SO_4 (≥ 99%), methanol (MeOH, ≥ 98%) and tert-butyl alcohol (TBA) were obtained from Aladdin Chemistry Co. Ltd., China. The stock solutions of $FeSO_4$ were freshly prepared each time, and $Na_2S_2O_8$ solution was stored for only one week.

Pre-oxidation and coagulation processes

The processes of generating $SO_4^{\cdot-}$ in Fe^{2+}/PS system are described as follows (Gu et al. 2017):

$$S_2O_8^{2-} + F_e^{2+} \rightarrow F_e^{3+} + 2SO_4^{\cdot-} \quad k = 2.0 \times 10^1\ M^{-1}\ S^{-1} \quad (1)$$

$$SO_4^{\cdot-} + F_e^{2+} \rightarrow F_e^{3+} + SO_4^{2-} \quad k = 4.6 \times 10^9\ M^{-1}\ S^{-1} \quad (2)$$

$$S_2O_8^{2-} + 2F_e^{2+} \rightarrow 2F_e^{3+} + 2SO_4^{2-} \quad k = 3.1 \times 10^4\ M^{-1}\ S^{-1} \quad (3)$$

It is worth noting that Fe^{2+} has the dual-functional capability of activator and coagulant in this work that pre-oxidation and coagulation can be completed at the same time.

The prepared *M. aeruginosa* suspension was added with desired amount of $Na_2S_2O_8$ and $FeSO_4$. Then, the suspension was mixed at 225 rpm for 6 min and subsequently at 40 rpm for 20 min, enabling a complete oxidation and coagulation, as shown by the Eqs. (1)–(3) that $SO_4^{\cdot-}$ for oxidation and Fe^{2+} for coagulation. Thereafter, the supernatants were taken out from 2 cm below the surface of water at specific time intervals and separated into a few of subsamples for further investigation of the reaction mechanisms. The cells settled down to the bottom were analyzed using scanning emission microscopy (SEM) and flow cytometry (Accuri C6, Becton Dickinson, USA). Given the limited effects on the *M. aeruginosa* cell removal, the impacts of co-existing anions (i.e., Cl^-, NO_3^- and HCO_3^-) from BG-11 media would not be further discussed in the following sections (Wang et al. 2016). Additionally, the quenching reaction by the scavenger of MeOH and TBA was conducted to determine the functional radicals.

Analytical methods

Removal efficiency of OD_{680} and chlorophyll-a

As the *M. aeruginosa* cell concentration was positively correlated with the optical density (OD) at 680 nm, the *M. aeruginosa* density was determined at wavelength of 680 nm using the spectrophotometer (U-3900, Hitachi, Japan). The removal efficiency of OD_{680} was calculated as follows.

$$R_{OD_{680}} = \frac{\left(OD_{680_i} - OD_{680_t}\right)}{OD_{680_i}} \times 100\% \quad (4)$$

where OD_{680_i} and OD_{680_t} were the algal OD at initial and time t (min), respectively.

Microcystis aeruginosa cell density was also linearly related to the content of chlorophyll-a, reflecting the primary productivity and photosynthesis ability of algal (Ni et al. 2015). The extracted chlorophyll-a (Chl-a) was determined by measuring the optical value at 649 nm and 665 nm with the spectrophotometer (U-3900, Hitachi, Japan) using ethanol (95%) solution. The content of Chl-a was calculated as follows (Sheng et al. 2019):

$$C_{\text{chl-a}} = 13.95A_{665} - 6.88A_{649} \quad (5)$$

The removal rate of chlorophyll-a was calculated by the change of Chl-a concentration as follows:

$$R_{\text{chla}} = \frac{(\text{chla}_i - \text{chla}_t)}{\text{chla}_i} \times 100\% \quad (6)$$

where chla_i and chla_t were the chlorophyll-a content at the initial time and time t (min), respectively.

Zeta potential and residual Fe

Zeta potential of *M. aeruginosa* suspensions was measured using the Zetasizer (Nano S90, Malvern, Britain) after slow mixing. The residual Fe was determined using an inductively coupled plasma optical emission spectrometer (ICP-OES, OPTIMA 8000, PerkinElmer, USA).

Dissolved organic carbon (DOC) and UV_{254}

The *M. aeruginosa* supernatant was filtered by a 0.45-μm cellulose acetate membrane (JIN TENG Technology CO., Ltd, China). Then, the TOC analyzer (Multi N/C 2100, JENA, Germany) and ultraviolet spectrometer (U-3900, Hitachi, Japan) were used to analyze the dissolved organic carbon (DOC) and UV_{254} of the *M. aeruginosa* supernatant.

Three-dimensional fluorescence excitation emission matrix (EEM) spectra

The fluorescence variation of AOM was analyzed using the three-dimensional fluorescence excitation emission matrix (EEM) spectrophotometer (F-7000, Hitachi, Japan). The scanning parameter of emission (Em) and the excitation (Ex) spectra matrices were in the range of 250–550 nm and 220–450 nm, respectively. Scan rate was set to 2400 nm/min at a gradient of 5 nm (Wang et al. 2016).

K^+ concentration and flow cytometer measurement

To evaluate the cell integrity, the concentration of K^+ released from *M. aeruginosa* cell was determined using the atomic absorption spectrometer (Shimadzu AA-7000, Japan) (Zhou et al. 2014). To assess the cellular activity, chlorophyll fluorescence of the precipitated cells by integrated Fe^{2+}/PS pre-oxidation and coagulation was determined using flow cytometry (Accuri C6, Becton Dickinson, USA).

Yellow fluorescence in channel FL2 (585 nm) was detected for chlorophyll content, and the flow rate was 20 µL/min.

Scanning electron microscopy (SEM)

The *M. aeruginosa* cells in the different samples were obtained at 4000 rpm for 10 min using centrifuge. After discarding the supernatant, the precipitated *M. aeruginosa* cells were mounted on copper stubs, coated with gold and examined under a SEM (VEGA TS 5136 MM, TESCAN Brno s.r.o, Czech Republic).

Extracellular and intracellular MCs

The MCs concentrations were determined by the enzyme-linked immunosorbent assay kit (Beacon Analytical Systems Inc, USA). The supernatant samples were extracted and then filtered with 0.45-µm cellulose acetate membrane (JIN TENG Technology CO., Ltd, China) to determine extracellular MCs. The other identical samples were for the total MCs analysis described by the previous methods (Bi et al. 2019). The intracellular MCs were obtained by the difference between total MCs and extracellular MCs.

Statistical analysis

Statistical analysis was performed using SPSS 19.0 (IBM, USA). One-way analysis of variance (ANOVA) was used to assess the variance with significance level of 5% ($P<0.05$). The error bar indicates the standard error of triplicate measurements. Different capital letters indicate significant differences.

Results and discussion

The effect on *M. aeruginosa* removal in the integrated pre-oxidation and coagulation

The lifetime of $SO_4^{\cdot-}$ radicals was $3–4\times10^{-5}$ s, while that of the $OH^{\cdot}$ radicals was only 2×10^{-8} s (Devi et al. 2016). As shown in Fig. 1, a two-stage reduction kinetics of *M. aeruginosa* in Fe^{2+}/PS system was observed with a rapid change in the initial 30 min and a stationary phase thereafter. Therefore, the settling time of 30 min was regarded as the optimum time for future research, which not only curtailed the treatment process but also reduced the risk of releasing undesirable compounds of IOM.

Figure 2 presents the removal efficiency of *M. aeruginosa* after settling for 30 min at different $FeSO_4$ concentrations. As $FeSO_4$ concentrations changed from 0.25 to 0.15 mmol/L, the removal efficiencies of OD_{680} and Chl-a increased from 4.80 to 98.8% and from 8.21 to 99.1%, respectively ($P<0.05$). However, after the $FeSO_4$ concentration increased to 0.10 mmol/L, the removal efficiencies of OD_{680} and Chl-a changed slightly. This was attributed to the fact that the amount of available $SO_4^{\cdot-}$ and $OH^{\cdot}$ contents decreased, resulting from the competitive reaction of overdose Fe^{2+} ions shown as follows (Liang et al. 2004; Neppolian et al. 2009).

$$Fe^{2+} + SO_4^{\cdot-} \rightarrow Fe^{3+} + SO_4^{2-} \quad (7)$$

$$Fe^{2+} + OH^{\cdot} \rightarrow Fe^{3+} + OH^{-} \quad (8)$$

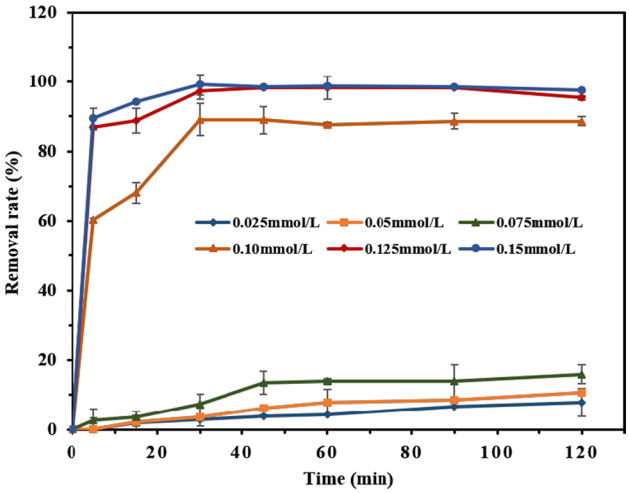

Fig. 1 Evolution of removal rate of OD_{680} over time by integrated Fe^{2+}/PS pre-oxidation and coagulation treatments in different $FeSO_4$ dosage systems. Data are presented as mean ± standard deviation ($n=3$)

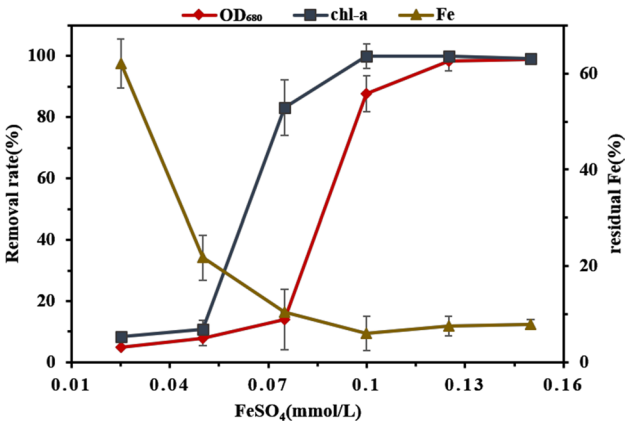

Fig. 2 Residual Fe and removal rate of OD_{680} and Chl-a of the *Microcystis* suspensions after settling 30 min under different $FeSO_4$ dosages. Data are presented as mean ± standard deviation ($n=3$)

Figure 2 also shows the change in the percentage of residual Fe. With the addition of $FeSO_4$, the percentage of residual Fe firstly decreased and then increased slightly when the dosage of $FeSO_4$ reached 0.10 mmol/L. The freshly produced in situ Fe (III) by hydrolyzation was significantly slower than the preformed Fe (III), leading to a superior reduction of *M. aeruginosa* (Ma et al. 2014). The insufficient generated Fe (III) hindered the massive aggregation of *M. aeruginosa* cells by adsorption bridging and charge neutralization. This finding corroborated the fact that *M. aeruginosa* was not removed efficiently with single 0.10 mmol/L $Na_2S_2O_8$, nor 0.10 mmol/L $FeSO_4$, as shown in Fig. S1. Therefore, the addition of 0.10 mmol/L $FeSO_4$ could simultaneously achieve a relatively high removal efficiency of *M. aeruginosa* and produce low residual Fe (0.24 mg/L), which was below the standard threshold of Fe content in drinking water (0.3 mg/L, GB5749-2006). Additionally, the optimal Fe^{2+}/PS mass ratio of 1:1 is observed in Fig. S2. The low Fe^{2+}/PS mass ratio was less effective for AOM degradation, while the excessive oxidants would cause the IOM release. Therefore, the best optimal conditions for controlling *M. aeruginosa* was determined to be 0.10 mmol/L $FeSO_4$ and 0.10 mmol/L $Na_2S_2O_8$. Moreover, the initial dosage of 0.10 mmol/L $Na_2S_2O_8$ (23.8 mg/L) had been far below the standard value of sulfate content in drinking water (250 mg/L, GB5749-2006).

Furthermore, it was noting that the optimal $FeSO_4$ dosage of 0.10 mmol/L and the Fe^{2+}/PS mass ratio of 1:1 in the present study was cost-effective compared to the previous studies (Wang et al. 2016; Jia et al. 2017). It has been reported that approximately 6 mmol/L sodium persulfate was consumed to achieve 98.2% removal efficiency of *M. aeruginosa* in the UV/persulfate process (Wang et al. 2016), while in the UV/H_2O_2 process, with the dosage of 0.375 mmol/L H_2O_2 and 0.125 mmol/L $FeSO_4$, a high *M. aeruginosa* removal efficiency of 94.7% was observed (Jia et al. 2017). However, the high cost of UV process would no doubt impede its wide application. Additionally, compared to Fe^{2+}/PS, other conventional coagulation methods also required high dosage of chemicals with high expenditure, such as 100 mg/L $FeCl_3$ (Li et al. 2015), 7.31 mg/L Chitosan (Pei et al. 2014) and 15 mg/L $AlCl_3$ (Sun et al. 2012). PACl has been reported to be a cost-effective coagulant with the dosage of 4 mg/L; however, a serious cell damage along with secondary environmental pollutions was observed (Sun et al. 2013). Therefore, Fe^{2+}/PS process was a promising method for removing *M. aeruginosa* and controlling cyanobacteria blooms in an environmentally friendly and cost- effective way.

The change of pH and zeta potential in the integrated pre-oxidation and coagulation

Table S1 presents the pH and zeta potentials of *M. aeruginosa* suspension under different $FeSO_4$ concentrations. The untreated *M. aeruginosa* cell possessed a relatively high negatively charged zeta potential of − 38.9 mV by the massive AOM. Subsequently, the zeta potentials of the cell increased to 3.27 mV along with the $FeSO_4$ dosage constantly changing from 0.25 to 0.15 mmol/L, and the pH value decreased. In comparison, the zeta potentials increased to − 30.15 mV and − 17.76 mV, respectively, when using 0.10 mmol/L $Na_2S_2O_8$ or 0.10 mmol/L $FeSO_4$ alone, and the pH changed slightly (Table S2), while a much higher value of − 0.814 mV was observed in the Fe^{2+}/PS system. The higher zeta potential observed in the Fe^{2+}/PS system was because the generated $SO_4^{\cdot-}$ oxidized negatively charged AOM and the formed in situ Fe (III), which was conducive to aggregating AOM and *M. aeruginosa* cells (Liu et al. 2017; Ma et al. 2012a, b). It was confirmed that the increased zeta potential of *M. aeruginosa* was the crucial reason for coagulation enhancement (Xie et al. 2016). Moreover, Liu et al. (2017) found that the zeta potential of *M. aeruginosa* cells was decreased significantly by pre-oxidation of ozone and permanganate, in which the negatively charged IOM was massively released due to cell rupture. However, this finding indicated that Fe^{2+}/PS was not likely to affect the cell structure, since the decrease in zeta potential caused by the released IOM was not observed.

AOM removal in the integrated pre-oxidation and coagulation

It has been well documented that lower concentrations of AOM could enhance coagulation via adsorption bridging effect (Xie et al. 2016). However, the extremely high levels of AOM would increase the negative charge of algal cells, resulting in coagulation suppression (Pivokonsky et al. 2006). Therefore, the oxidation of AOM was considered as a crucial step for enhancing the removal of *M. aeruginosa*.

The DOC and UV_{254} decreased sharply ($P < 0.05$) along with $FeSO_4$ addition, as shown in Fig. 3. The Fe^{2+} activated $Na_2S_2O_8$ to generate $SO_4^{\cdot-}$ for AOM degradation in the pre-oxidation, and simultaneously, the in situ formed Fe (III) aggregated *M. aeruginosa* cells as well as AOM, along with the changes in *M. aeruginosa* removal and residual Fe (Fig. 2). Furthermore, the declining trend of DOC indicated that Fe^{2+}/PS caused limited damage to the *M. aeruginosa* cell walls. Else, the DOC level would increase significantly, due to the released IOM and internal metabolites caused by cell lysis (Zhou et al. 2014). The unsaturated carbon bonds and aromatic structures of the organic compound can be reflected by UV_{254} (Liu et al. 2017). The newly formed in situ Fe (III), derived from the pre-oxidation of Fe^{2+}, showed better performance of AOM degradation compared to preformed Fe (III), particularly those with unsaturated structures (Ma et al. 2014). Therefore, the decline of UV_{254} in Fig. 3 affirmed the reaction between Fe (III) and organics

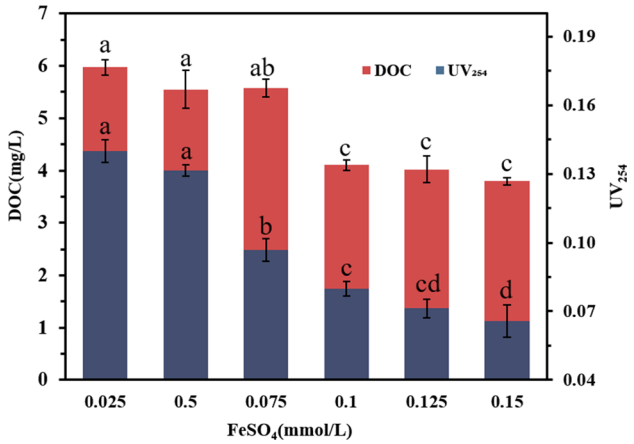

Fig. 3 Mineralization of organic matters after settling 30 min under different $FeSO_4$ dosage. Data are presented as mean ± standard deviation ($n = 3$)

with unsaturated carbon chains, such as humic acid (Silvia et al. 2010) or protein (Ma et al. 2016; Pivokonsky et al. 2012), which was pivotal step for *M. aeruginosa* removal.

EEM spectra of extracellular AOM

Three-dimensional EEM was employed for further investigation of chemical composition of the extracellular AOM in Fe^{2+}/PS process. Four fluorescence peaks were identified, as shown in Fig. 4a–e. Peak A at Ex/Em of 270/442 nm and peak C at 350/432 nm were associated with fulvic- and humic-like substances, respectively. Peak T1 (280/330 nm) and peak T2 (230/330 nm) were related to dissolved microbial metabolites and protein-like compounds, respectively (Coble 1996; Hudson et al. 2007). High intensities of Peak T1 and T2 were observed in the control (Fig. 4a), suggesting that AOM contained a higher concentration of dissolved microbial metabolites and protein-like substances (Huang et al. 2014; Ou et al. 2011). It was found that protein-like substances were relatively easy to be decomposed during pre-oxidation treatment process. Therefore, as shown in Fig. 4c, almost all protein-like components and a part of dissolved microbial metabolites were oxidized. The protein-like substances, with better hydrophilicity and poor aggregation ability, were preferentially oxidized by free radicals (Tian et al. 2018). However, as the concentrations of $FeSO_4$ were increased to 0.125 mmol/L, the intensity of peaks A and C was significantly increased, along with the weakened intensity of peaks T1 and disappearance of peak T2 in contrast (Fig. 4e). The *M. aeruginosa* cells were under chemical or physiological stress during the coagulation process (Khatoon et al. 2018; Ma et al. 2016), which may accelerate the secretion of the fulvic- and humic-like substances and release IOM due to cell lysis. These results well explained the declining tendency of DOC and UV_{254} observed in Fig. 3 and demonstrated that the free radicals were relatively easy to react with protein-like substances and dissolved microbial metabolites containing greater unsaturated bonds. As shown in Fig. S3, the AOM changed slightly in single $Na_2S_2O_8$ or $FeSO_4$ system, resulting in poor *M. aeruginosa* removal. This finding indicated that a decisive process of removing *M. aeruginosa* was to generate free radical for pre-oxidation.

The role of free radicals in *M. aeruginosa* removal was further investigated. Table S3 shows the *M. aeruginosa* removal efficiencies with MeOH and TBA co-existed in Fe^{2+}/PS system. This result showed that the inhibition degree caused by MeOH was greater than TBA, but the whole reaction was not completely suppressed. MeOH and TBA transformed the degradation and mineralization process of *M. aeruginosa* by quenching the useful free radical. Both $SO_4^{\cdot-}$ and $OH^{\cdot}$ ould be effectively inhibited by the scavenger of MeOH, while TBA was only effective for $OH^{\cdot}$ inhibition OH (Wang et al. 2016). This phenomenon implied that both $SO_4^{\cdot-}$ and $OH^{\cdot}$ were responsible for oxidizing *M. aeruginosa* cells in this work.

Cell viability

Figure 5 shows the chlorophyll fluorescence intensity of the *M. aeruginosa* cell flocs measured by flow cytometry. *M. aeruginosa* possesses Chl-a auto-fluorescence, and its intensity is positively correlated with chlorophyll content, which can reflect the cellular activity (Hyka et al. 2013). Both the proportion of *M. aeruginosa* cells with higher activity and chlorophyll fluorescence intensity decreased with higher $FeSO_4$ dosage (Fig. 5). Potassium (K) was one of the significant elements for maintaining cell osmotic pressure and reflected cell membrane integrity (Gu et al. 2017). As shown in Fig. S4, with increased $FeSO_4$ concentration, the K^+ released from intracellular fluid increased significantly ($P < 0.05$). Jia et al. (2017) reported that after H_2O_2 treatment, only small amounts of cells were damaged with approximately 50% K^+ released. In the present study, under optimal dosage of 0.10 mmol/L $FeSO_4$, only 42% K^+ was released from *M. aeruginosa*, and consequently, the majority of *M. aeruginosa* cells remained intact. Additionally, under the optimal level, the cell percentage of high activity only decreased 15.64% compared to the controls, implying that only small amounts of *M. aeruginosa* cell membrane might have been impaired in Fe^{2+}/PS process.

Physiology morphology of *M. aeruginosa* cells

In order to further investigate the cell membranes integrity under optimum dosage of $FeSO_4$ and $Na_2S_2O_8$, the surface morphology of *M. aeruginosa* cells before and after Fe^{2+}/PS treatment is shown in Fig. 6 by SEM. The *M.*

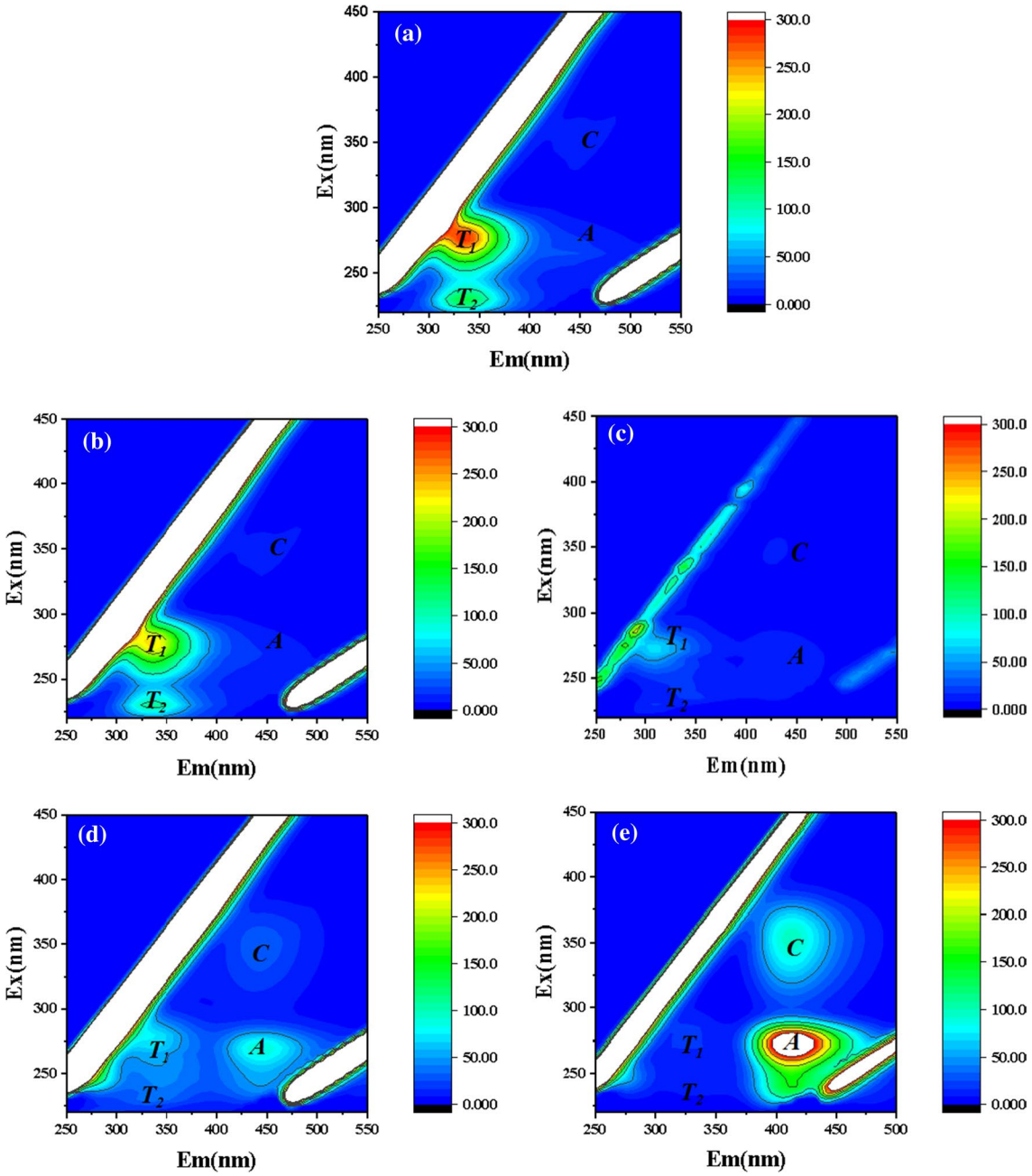

Fig. 4 Fluorescence EEM spectra of extracellular AOM. **a** Control, **b** 0.05 mmol/L $FeSO_4$, **c** 0.075 mmol/L $FeSO_4$, **d** 0.10 mmol/L $FeSO_4$, **e** 0.125 mmol/L $FeSO_4$

aeruginosa cells in control systems (Fig. 6a) were smooth, and some secretions were observed, presumably due to the naturally released metabolites (Jia et al. 2017). After the addition of optimal Fe^{2+}/PS dosage, a small amount of *M. aeruginosa* cells tended to wrinkle, and the surface morphologies were moderately altered without the leakage of cell inclusion (Fig. 6b), which was in accordance with the K^+ release in Fig. S4. This might have attributed to the increase in the extracellular polymeric substances (EPSs) produced by *M. aeruginosa*, enhancing the formation of the protective shield for *M. aeruginosa* cells against the external stress (Zhao et al. 2011). However, if the Fe^{2+}/PS dosage increased, the protective barrier provided by EPS would be weakened and diminished. This result indicated that only a small scale of algal cell membranes was damaged in the Fe^{2+}/PS process, and the majority of *M. aeruginosa* cells, however, still remained integrated and spherical.

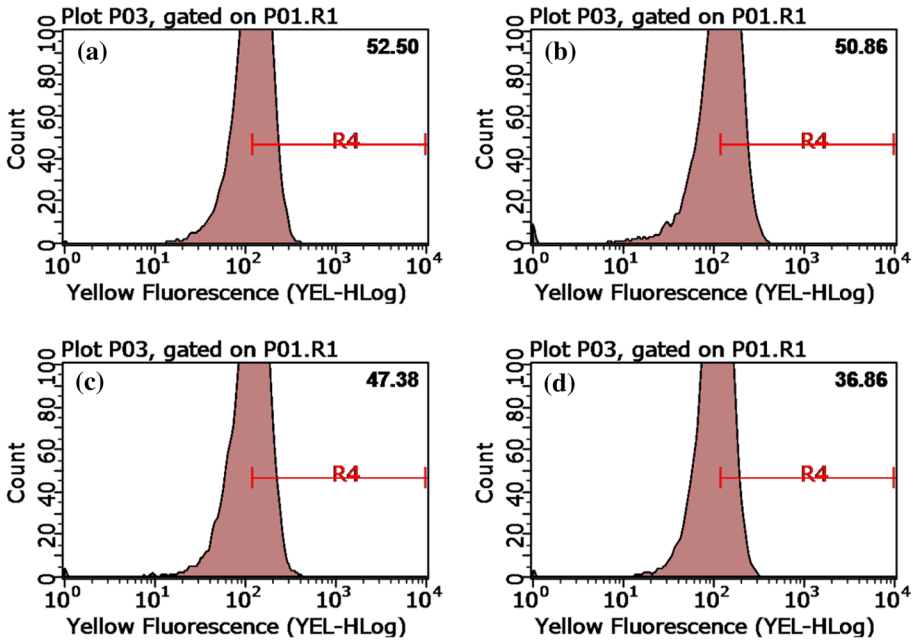

Fig. 5 Chlorophyll fluorescence of the Microcystis after settling 30 min. **a** Control, **b** 0.025 mmol/L $FeSO_4$, **c** 0.075 mmol/L $FeSO_4$, **d** 0.10 mmol/L $FeSO_4$

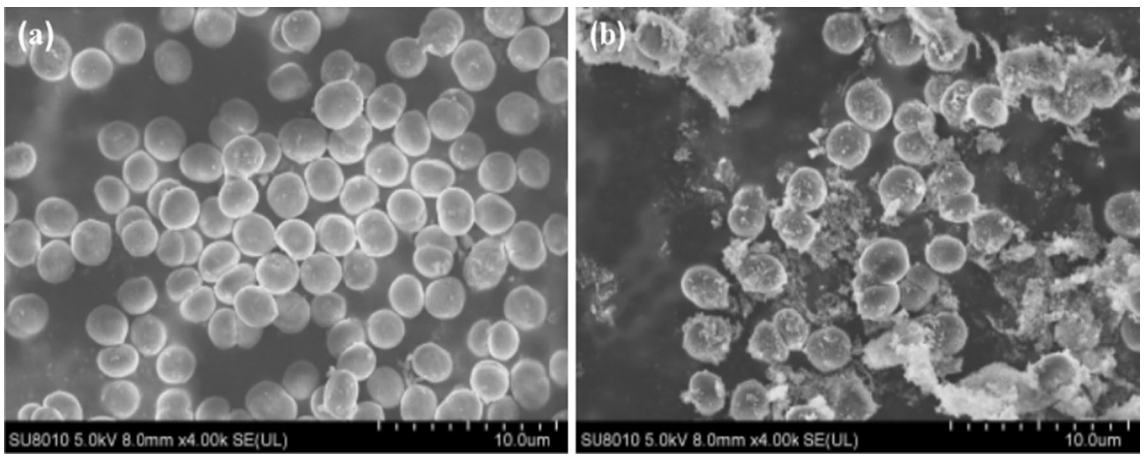

Fig. 6 The SEM images of surface morphology of *M. aeruginosa* cells **a** before, **b** after 30-min settling by Fe^{2+}/PS pre-oxidation and coagulation treatments

The release of microcystins (MCs) in the integrated pre-oxidation and coagulation

Given the fact that the MCs are highly toxic, the change in microcystins is presented in Fig. 7. As $FeSO_4$ dosage increased from 0.025 to 0.10 mmol/L, the extracellular MCs decreased significantly ($P < 0.05$), while the change in intracellular MCs was not obvious ($P > 0.05$), implying that most *M. aeruginosa* cells were intact. However, the intracellular MCs decreased remarkably and the extracellular MCs increased slightly, when the $FeSO_4$ dosage reached 0.125 mmol/L. The *M. aeruginosa* cells lysis occurred, and numerous intracellular MCs were released from *M. aeruginosa* cells under this condition. However, the content of sulfate radical was high and high removal of MCs was observed. Compared to 0.10 mmol/L $FeSO_4$, the concentrations of extracellular MCs declined slightly at the concentration of 0.15 mmol/L. This finding indicated that the degradation rate of MCs by sulfate radical was greater than the release rate of MCs from *M. aeruginosa* cells.

Wang et al. (2016) reported that the structure of *M. aeruginosa* cells was completely out of shape after the 120-min treatment by UV/PS systems. Slight damage of the spherical surface occurred during the UV/H_2O_2 pre-oxidation process. However, additional coagulants were needed along with the costs incurred. Although there was no evident alteration in *M. aeruginosa* cell morphology after ferrate (VI) oxidation, the removal efficiency of *M.*

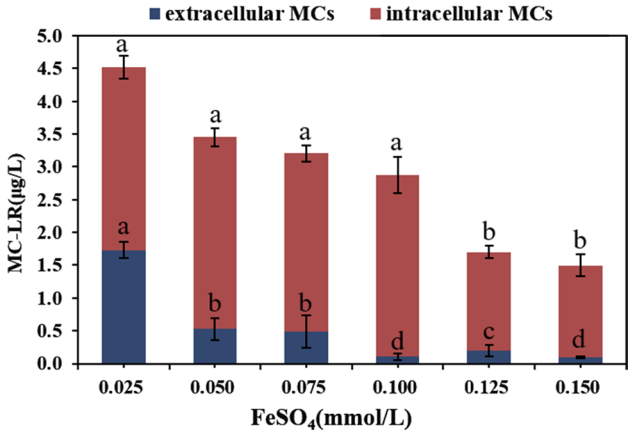

Fig. 7 The concentrations of intracellular and extracellular MCs after 30-min settling under different $FeSO_4$ dosages. Data are presented as mean ± standard deviation ($n = 3$)

aeruginosa was relatively poor (Zhou et al. 2014). Therefore, compared to these previous studies, the Fe^{2+}/PS process is not only effective in removing *M. aeruginosa* cells without additional coagulants, but also reliable in reducing the risk of secondary pollution, resulting from the better control of the microcystins.

Conclusion

This study demonstrated that the Fe^{2+}/PS process was a highly effective method for removing *M. aeruginosa* cells and AOM via in situ Fe (III) formed. The generated $SO_4^{\cdot-}$ and $OH^{\cdot}$ were both responsible for the efficient degradation of AOM. Moreover, the dissolved microbial metabolites and protein-like substances seemed more susceptible to be oxidized, and subsequently, the coagulation process was significantly enhanced. Fe^{2+}/PS process has been proved to be highly efficient in removing *M. aeruginosa* cells and AOM, due to in situ formed Fe (III) without the additional coagulants. SEM image indicated that the optimal Fe^{2+}/PS ratio reduced the cyanobacterial cell damage and MCs had been well controlled, preventing from the risk of secondary pollution. Therefore, it is concluded that Fe^{2+}/PS process is a promising and environmental-friendly solution to the problems associated with cyanobacteria blooming.

Acknowledgements This work was financially supported by the Natural Science Foundation of Guangdong Province (No. 2017A030313239), Research Project of Sino-Singapore international joint research institute (No. 202-A018001), National Key Research and Development Program of China (N0. 2019YFA0210400), the Ministry of Science and Technology of China for State Key Research and Development Project (No. 2016YFC04007082) and the Science and Technology Planning Project of Maoming, China (No. 2019S002).

References

Ahmed MM, Barbati S, Doumenq P, Chiron S (2012) Sulfate radical anion oxidation of diclofenac and sulfamethoxazole for water decontamination. Chem Eng J 197(14):440–447

Bi X, Dai W, Wang X, Dong S, Zhang S, Zhang D, Wu M (2019) Microcystins distribution, bioaccumulation, and *Microcystis* genotype succession in a fish culture pond. Sci Total Environ 688:380–388

Coble PG (1996) Characterization of marine and terrestrial DOM in seawater using excitation-emission matrix spectroscopy. Mar Chem 51(4):325–346

Devi P, Das U, Dalai AK (2016) In-situ chemical oxidation: Principle and applications of peroxide and persulfate treatments in wastewater systems. Sci Total Environ 571:643–657

Gu N, Wu Y, Gao J, Meng X, Zhao P, Qin H, Wang K (2017) *Microcystis aeruginosa* removal by in situ chemical oxidation using persulfate activated by Fe^{2+} ions. Ecol Eng 99:290–297

He X, Wert EC (2016) Colonial cell disaggregation and intracellular microcystin release following chlorination of naturally occurring *Microcystis*. Water Res 101:10–16

Henderson R, Parsons SA, Jefferson B (2008) The impact of algal properties and pre-oxidation on solid–liquid separation of algae. Water Res 42(8–9):1827–1845

Hisao H, Yumiko N, Misako M, Shuzo K (2008) Efficient decomposition of perfluorocarboxylic acids and alternative fluorochemical surfactants in hot water. Environ Sci Technol 42(19):7438–7443

Huang W, Chu H, Dong B, Liu J (2014) Evaluation of different algogenic organic matters on the fouling of microfiltration membranes. Desalination 344(344):329–338

Hudson N, Baker A, Reynolds D (2007) Fluorescence analysis of dissolved organic matter in natural, waste and polluted waters: a review. River Res Appl 23(6):631–649

Hyka P, Lickova S, Pribyl P, Melzoch K, Kovar K (2013) Flow cytometry for the development of biotechnological processes with microalgae. Biotechnol Adv 31(1):2–16

Jia P, Zhou Y, Zhang X, Zhang Y, Dai R (2017) Cyanobacterium removal and control of algal organic matter (AOM) release by UV/H_2O_2 pre-oxidation enhanced Fe (II) coagulation. Water Res 131:122–130

Khatoon H, Kok Leong L, Abdu Rahman N, Mian S, Begum H, Banerjee S, Endut A (2018) Effects of different light source and media on growth and production of phycobiliprotein from freshwater cyanobacteria. Bioresour Technol 249:652–658

Kwon M, Kim S, Yoon Y, Jung Y, Hwang TM, Lee J et al (2015) Comparative evaluation of ibuprofen removal by UV/H_2O_2 and $UV/S_2O_8^{2-}$ processes for wastewater treatment. Chem Eng J 269(3):379–390

Lei L, Naiyun G, Yang D, Juanjuan Y, Kejia Z (2012) Characterization of intracellular and extracellular algae organic matters (AOM) of *Microcystic aeruginosa* and formation of AOM-associated disinfection byproducts and odor and taste compounds. Water Res 46(4):1233–1240

Li X, Pei H, Hu W, Meng P, Sun F, Ma G, Xu X, Li Y (2015) The fate of *Microcystis aeruginosa* cells during the ferric chloride coagulation and flocs storage processes. Environ Technol 36(5–8):920–928

Liang C, Bruell CJ, Marley MC, Sperry KL (2004) Persulfate oxidation for in situ remediation of TCE. I. Activated by ferrous ion with and without a persulfate-thiosulfate redox couple. Chemosphere 55(9):1213–1223

Liu B, Qu F, Chen W, Liang H, Wang T, Cheng X, Yu H, Li G, Van der Bruggen B (2017) *Microcystis aeruginosa*-laden water treatment using enhanced coagulation by persulfate/Fe (II), ozone

and permanganate: comparison of the simultaneous and successive oxidant dosing strategy. Water Res 125:72–80

Ma M, Liu R, Liu H, Qu J (2012a) Chlorination of *Microcystis aeruginosa* suspension: cell lysis, toxin release and degradation. J Hazard Mater 217–218(3):279–285

Ma M, Liu R, Liu H, Qu J (2012b) Effect of moderate pre-oxidation on the removal of *Microcystis aeruginosa* by $KMnO_4$-Fe (II) process: significance of the in-situ formed Fe (III). Water Res 46(1):73–81

Ma M, Liu R, Liu H, Qu J (2014) Mn (VII)-Fe (II) pre-treatment for *Microcystis aeruginosa* removal by Al coagulation: simultaneous enhanced cyanobacterium removal and residual coagulant control. Water Res 65:73–84

Ma C, Pei H, Hu W, Xu H, Jin Y (2016) The lysis and regrowth of toxic cyanobacteria during storage of achitosan–aluminium chloride composite coagulated sludge: implications for drinking water sludge treatment. RSC Adv 6(114):112756–112764

Mahdiahmed M, Chiron S (2014) Ciprofloxacin oxidation by UV-C activated peroxymonosulfate in wastewater. J Hazard Mater 265:41–46

Min Y, Jianwei Y, Zonglai L, Zhaohai G, Michael B, Tsair-Fuh L (2008) Taihu Lake not to blame for Wuxi's woes. Science 319(5860):158–158

Neppolian B, Doronila A, Grieser F, Ashokkumar M (2009) Simple and efficient sonochemical method for the oxidation of Arsenic (III) to Arsenic(V). Environ Sci Technol 43(17):6793

Ni L, Jie X, Wang P, Li S, Wang G, Li Y, Li Y, Acharya K (2015) Effect of linoleic acid sustained-release microspheres on *Microcystis aeruginosa* antioxidant enzymes activity and microcystins production and release. Chemosphere 121:110–116

Ou H, Gao N, Deng Y, Qiao J, Zhang K, Li T, Dong L (2011) Mechanistic studies of *Microcystic aeruginosa* inactivation and degradation by UV-C irradiation and chlorination with poly-synchronous analyses. Desalination 272(1):107–119

Paerl HW, Paul VJ (2012) Climate change: links to global expansion of harmful cyanobacteria. Water Res 46(5):1349–1363

Pei HY, Ma CX, Hu WR, Sun F (2014) The behaviors of *Microcystis aeruginosa* cells and extracellular microcystins during chitosan flocculation and flocs storage processes. Bioresour Technol 151(1):314–322

Pieterse AJH, Cloot A (1997) Algal cells and coagulation, flocculation and sedimentation processes. Water Sci Technol 36(4):111–118

Pivokonsky M, Kloucek O, Pivokonska L (2006) Evaluation of the production, composition and aluminum and iron complexation of algogenic organic matter. Water Res 40(16):3045–3052

Pivokonsky M, Safarikova J, Bubakova P, Pivokonska L (2012) Coagulation of peptides and proteins produced by *Microcystis aeruginosa*: interaction mechanisms and the effect of Fe-peptide/protein complexes formation. Water Res 46(17):5583–5590

Qi C, Liu X, Ma J, Lin C, Li X, Zhang H (2016) Activation of peroxymonosulfate by base: implications for the degradation of organic pollutants. Chemosphere 151:280–288

Rodriguez S, Vasquez L, Costa D, Romero A, Santos A (2014) Oxidation of orange G by persulfate activated by Fe (II), Fe (III) and zero valent iron (ZVI). Chemosphere 101(3):86–92

Silvia B, Muller FOLL, Kuei-Chen C, Chon-Lin L (2010) Evidence for strong but dynamic iron-humic colloidal associations in humic-rich coastal waters. Environ Sci Technol 44(22):8485–8490

Sheng H, Niu X, Song Q, Li Y, Zhang R, Zou D, Lai S, Yang Z, Tang Z, Zhou S (2019) Physiological and biochemical responses of *Microcystis aeruginosa* to phosphine. Environ Pollut 247:165–171

Sun F, Pei H-Y, Hu W-R, Ma C-X (2012) The lysis of *Microcystis aeruginosa* in $AlCl_3$ coagulation and sedimentation processes. Chem Eng J 193–194:196–202

Sun F, Pei HY, Hu WR et al (2013) The cell damage of Microcystis aeruginosa in PACl coagulation and floc storage processes. Sep Purif Technol 115:123–128

Svrcek C, Smith DW (2004) Cyanobacteria toxins and the current state of knowledge on water treat. J Environ Eng Sci 3(3):155–185

Teixeira MR, Rosa MJ (2006) Comparing dissolved air flotation and conventional sedimentation to remove cyanobacterial cells of *Microcystis aeruginosa*: part I: the key operating conditions. Sep Purif Technol 52(1):84–94

Tian J, Wu C, Yu H, Gao S, Li G, Cui F, Qu F (2018) Applying ultraviolet/persulfate (UV/PS) pre-oxidation for controlling ultrafiltration membrane fouling by natural organic matter (NOM) in surface water. Water Res 132:190–199

Wang J, Wang S (2018) Activation of persulfate (PS) and peroxymonosulfate (PMS) and application for the degradation of emerging contaminants. Chem Eng J 334:1502–1517

Wang Z, Chen Y, Xie P, Shang R, Ma J (2016) Removal of *Microcystis aeruginosa* by UV-activated persulfate: performance and characteristics. Chem Eng J 300:245–253

Xie P, Chen Y, Ma J, Zhang X, Zou J, Wang Z (2016) A mini review of preoxidation to improve coagulation. Chemosphere 155:550–563

Zhao X, Zhang Y (2011) Algae-removing and algicidal efficiencies of polydiallyldimethylammonium chloride composite coagulants in enhanced coagulation treatment of algae-containing raw water. Chem Eng J 173(1):164–170

Zhao L, Lin L, Ming L, Xu Z, Wei Z (2011) Effects of Ca and Mg levels on colony formation and EPS content of cultured *M. aeruginosa*. Procedia Environ Sci 10:1452–1458

Zhou J, Liu J, Gao N, Zhao Z, Li L, Peng W, Cui F (2020) *Microcystis aeruginosa*-laden water treatment using peroxymonosulfate enhanced Fe (II) coagulation: performance and the role of in situ formed Fe_3O_4. Chem Eng J 382:123012

Zhou S, Shao Y, Gao N, Zhu S, Li L, Deng J, Zhu M (2014) Removal of *Microcystis aeruginosa* by potassium ferrate (VI): impacts on cells integrity, intracellular organic matter release and disinfection by-products formation. Chem Eng J 251:304–309